

Anderson localization of a Majorana fermion

D. A. Ivanov,^{1,2} P. M. Ostrovsky,^{3,4} and M. A. Skvortsov^{4,5}

¹*Institute for Theoretical Physics, ETH Zürich, 8093 Zürich, Switzerland*

²*Institute for Theoretical Physics, University of Zürich, 8057 Zürich, Switzerland*

³*Max Planck Institute for Solid State Research, Heisenbergstr. 1, 70569 Stuttgart, Germany*

⁴*L. D. Landau Institute for Theoretical Physics, 142432 Chernogolovka, Russia*

⁵*Moscow Institute of Physics and Technology, 141700 Moscow, Russia*

(Dated: June 29, 2013)

Isolated Majorana fermion states can be produced at the boundary of a topological superconductor in a quasi-one-dimensional geometry. If such a superconductor is connected to a disordered quantum wire, the Majorana fermion is spread into the wire, subject to Anderson localization. We study this effect in the limit of a thick wire with broken time-reversal and spin-rotational symmetries. With the use of a supersymmetric nonlinear sigma model, we calculate the average local density of states in the wire as a function of energy and of the distance from the interface with the superconductor. Our results may be qualitatively explained by the repulsion of states from the Majorana level and by Mott hybridization of localized states.

1. Introduction.— In recent years, search for Majorana electron levels in solid-state systems has intensified, motivated by their potential use in quantum computing [1]. Several experimental groups reported indications of Majorana fermions in hybrid superconductor-semiconductor systems [2–5], which further stimulated theoretical studies of Majorana fermions in superconducting proximity structures. One of the interesting theoretical questions relevant for the analysis of the recent experiments is the role of disorder in the structure of the electronic spectrum of systems with Majorana fermions. This topic was subject of several recent papers, which addressed transport properties of hybrid systems with Majorana states [6–9].

An alternative approach to disordered systems is in terms of correlation functions, the simplest of which is the average local density of states (LDOS). If the disorder is strong enough, the electronic states are localized [10], including the Majorana fermion. At the same time, the LDOS at low energies is modified, due to the level repulsion from the Majorana state (this effect was studied in detail in the zero-dimensional random-matrix limit [11, 12]). In the case of a thick quasi-one-dimensional wire with a large number of channels, the modification of the density of states in the presence of a localized Majorana level can be accessed with the use of a supersymmetric nonlinear sigma model [13]. This approach was developed in Ref. 14 for the case of a non-topological superconducting system without Majorana fermion.

In the present paper, we adapt the calculation of Ref. 14 to the case of a hybrid system consisting of a topological superconductor with a Majorana level and a wire with both time-reversal and spin symmetries broken. As a result, we find the spatial structure of the localized Majorana state and the modification of the density of states at low energies due to the level repulsion from the Majorana level. The localization of the Majorana level is similar to the localization of states in the bulk of the

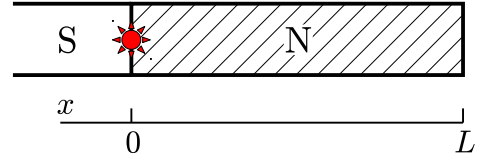


FIG. 1: (Color online) A disordered quantum wire (N) of length L coupled to a topological superconductor (S) at $x = 0$. The star marks the location of a Majorana fermion state. This state spreads at the localization length scale ξ into the wire and at the superconducting coherence length (which is assumed to be much shorter than ξ) into the superconductor.

wire, and its level-repulsion effect extends to the Mott length scale. We further explain our results in terms of the Mott hybridization of localized states [15, 16] and compare our findings to those in Ref. 14.

2. Model.— The model we consider is identical to that described in Ref. 14, with the only difference that the superconductor is now of a topological type hosting a Majorana fermion at the interface with the normal metal [17]. The setup is schematically shown in Fig. 1. The wire has length L and the number of channels $N \gg 1$. Both the spin-rotational and time-reversal symmetry are assumed to be broken in the wire (at the length scales shorter than all other length scales of the theory). It therefore belongs to the symmetry class A (in Cartan notation [18]) and to the model IIb in Efetov’s classification [19]. The superconductor is also assumed to have both time-reversal and spin-rotational symmetry broken and to be in a topological phase [17]. This superconducting symmetry class is usually denoted as B, D or BD [11, 12, 18, 20]. We prefer to call this symmetry class B to emphasize the presence of a Majorana state at the boundary. An example of a microscopic Hamiltonian leading to such a symmetry can be found in Refs. 21, 22.

We assume quantum coherence in the wire, which leads to Anderson localization at the localization length

$\xi = 2\pi\nu AD$ (here D is the diffusion coefficient in the wire, ν is the density of states, and A is the wire cross section). Localization in the wire defines the energy scale $\Delta_\xi = D/\xi^2$ (of the order of the level spacing and of the Thouless energy at the length ξ). In short wires ($L \ll \xi$), another energy scale comes into play: the level spacing in the wire, $\delta = (2\nu AL)^{-1}$ [23]. The localization of the Majorana fermion and the related level-repulsion effects occur at distances $x \lesssim \xi$ from the interface [up to logarithmic corrections, see the discussion of the Mott length (12) below] and at energies $E \lesssim \max(\Delta_\xi, \delta)$ around the Fermi level, as in the non-topological case [14]. We further assume these conditions on x and E .

The interface between such a superconductor and a wire may be described in terms of a scattering matrix $2N \times 2N$, which involves both normal and Andreev reflections. We assume a large total Andreev conductance. Additionally, we assume that the gap in the superconducting part of the junction is much larger than the energy scales Δ_ξ and δ . Then, within the window of energies considered, we may neglect the energy dependence of the Andreev scattering matrix (the limit of a broad ‘‘Majorana resonance’’ [24, 25]). The symmetry properties of such a scattering matrix are discussed in detail in Refs. 6, 9, 17. Similarly to the results of Ref. 14, we find that the role of the Andreev interface, in this high-transparency limit, is to fully suppress the soft localization modes (diffusons and cooperons) incompatible with the symmetry of the superconductor. At such an interface, the boundary conditions for the supersymmetric nonlinear sigma model describing the wire take a particularly simple form (see the following section).

3. Density of states: general formalism.— Our main object of study is the disorder-averaged local density of states $\langle \rho_E(x) \rangle$ (normalized to the bulk value in the wire). Following the procedure described in Ref. 14, we express it as an expectation value in a supersymmetric nonlinear sigma model [19],

$$\langle \rho_E(x) \rangle = \frac{1}{4} \text{Re} \int \text{str} (k \Lambda Q(x)) e^{-S[Q]} DQ. \quad (1)$$

Here Q is the supersymmetric 4×4 matrix acting in the product of the Fermi-Bose (FB) and retarded-advanced (RA) two-dimensional spaces and subject to the constraint $Q^2 = 1$ (this space of Q matrices corresponds to the symmetry class A [18]). The matrix $\Lambda = \sigma_z^{\text{RA}}$ is the metallic saddle point of the sigma model, and the supersymmetry-breaking matrix k is defined as $k = \sigma_z^{\text{FB}}$ (we follow the notations of Ref. [19]). The supersymmetric action has the form

$$S[Q] = \frac{\pi\nu A}{4} \int dx \text{str} [D(\nabla Q)^2 + 4iE\Lambda Q]. \quad (2)$$

The boundary conditions on the matrix Q are free at the end point $x = L$. At the interface with the superconductor, under the assumptions specified in the previous

section, the matrix Q is restricted to the symmetry class of the combination of the symmetries in the wire and in the superconductor (class B in our case).

As usual, we parameterize the Q matrix by the eigenvalues of its RR block, which are conventionally denoted λ_F and λ_B (for the fermionic and bosonic eigenvalues, respectively) [19]. The fermionic parameter λ_F takes values between -1 and 1 (compact), and the bosonic component λ_B between 1 and $+\infty$ (noncompact). At the interface with a superconductor, the Q matrix is reduced to that of the symmetry class B or D (depending on the presence or absence of a Majorana level), which constrains the FF block to two points only: $\lambda_F = \pm 1$ [11, 12, 14]. As derived in Ref. 14, in the case of class D (no Majorana level), the two components of the functional integral (1) corresponding to $\lambda_F(x=0) = 1$ and $\lambda_F(x=0) = -1$ must be added with opposite signs. In Ref. 12, it was remarked that the difference between the presence and absence of the Majorana mode corresponds to reversing the relative sign between the functional integrals over the two disconnected components of the space of Q matrices. Therefore, we conclude that, in the case of class B (with the Majorana mode), the average density of states is given by reversing the relative sign in Eq. (28) of Ref. 14:

$$\langle \rho_E(x) \rangle = 1 + \text{Re} \int_1^\infty d\lambda_B \frac{\Psi(1, \lambda_B; x) + \Psi(-1, \lambda_B; x)}{2}, \quad (3)$$

with the wave function $\Psi(\lambda_F, \lambda_B; x)$ defined as [26–28]

$$\begin{aligned} \Psi(\lambda_F, \lambda_B; x) \\ = e^{-2\tilde{H}x/\xi} (\lambda_B - \lambda_F) e^{-2\tilde{H}(L-x)/\xi} (\lambda_B - \lambda_F)^{-1}. \end{aligned} \quad (4)$$

The Hamiltonian \tilde{H} governing the evolution of the wave function is given by

$$\tilde{H} = \tilde{H}_B + \tilde{H}_F, \quad (5)$$

where

$$\tilde{H}_B = -\frac{1}{2} \frac{\partial}{\partial \lambda_B} (\lambda_B^2 - 1) \frac{\partial}{\partial \lambda_B} + \frac{\kappa^2}{16} \lambda_B, \quad (6a)$$

$$\tilde{H}_F = -\frac{1}{2} \frac{\partial}{\partial \lambda_F} (1 - \lambda_F^2) \frac{\partial}{\partial \lambda_F} - \frac{\kappa^2}{16} \lambda_F, \quad (6b)$$

and we define $\kappa^2 = -8iE/\Delta_\xi$.

4. Short-wire limit.— In the limit of a short wire, $L \ll \min(\xi, \sqrt{D/E})$, the gradient terms in the Hamiltonian (5) may be neglected [14], and a simple calculation leads to the well-known result for the random-matrix ensemble of class B [12, 29]:

$$\langle \rho_E(x) \rangle = 1 - \frac{\sin(2\pi E/\delta)}{(2\pi E/\delta)} + \delta(E/\delta). \quad (7)$$

The Majorana level reveals itself as a delta-function term in the density of states. The integral weight of this delta peak equals $1/2$, which reflects the Majorana nature of this electronic level.

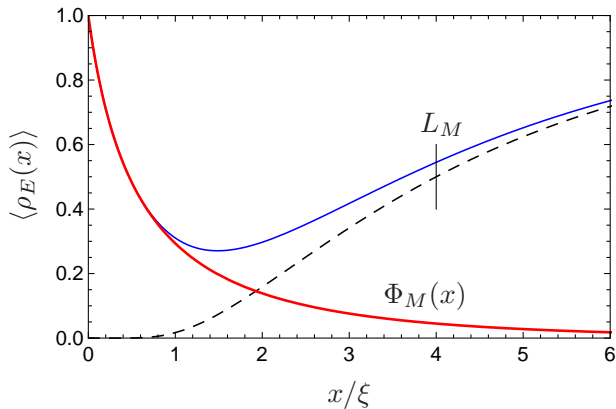


FIG. 2: (Color online) Sketch of the average LDOS $\langle \rho_E(x) \rangle$ in the infinite-wire limit ($L \rightarrow \infty$) at a small finite energy E as a function of x (thin blue curve), as given by Eq. (10). Close to the interface, it follows the profile of the Majorana mode $\Phi_M(x)$ (thick red curve). At $x \sim L_M$, the LDOS exhibits a crossover given by the erf function (dashed black line).

5. *Infinite-wire limit.*— In the limit of an infinite wire, at low energies ($E \ll \Delta_\xi$), the calculation can be performed using the technique developed in Ref. 28. Taking the limit $L \rightarrow \infty$ in Eq. (4) results in

$$\Psi(\lambda_F, \lambda_B; x)_{L \rightarrow \infty} = e^{-2(\tilde{H}_F + \tilde{H}_B)x/\xi} \Psi_0(\lambda_F, \lambda_B), \quad (8)$$

where

$$\Psi_0(\lambda_F, \lambda_B) = I_0(q) p K_1(p) + q I_1(q) K_0(p) \quad (9)$$

(with $p = \kappa \sqrt{(\lambda_B + 1)/2}$ and $q = \kappa \sqrt{(\lambda_F + 1)/2}$) is the zero mode of the one-dimensional sigma model in the unitary symmetry class found in Ref. 30.

Since the bosonic and fermionic degrees of freedom separate, the calculation may be further performed perturbatively in the fermionic sector (using the assumption of $E \ll \Delta_\xi$) and by expanding in the basis of eigenstates of \tilde{H}_B in the bosonic sector [28]. The details of the calculation can be found in the Supplemental Material [31]. The result has the form

$$\langle \rho_E(x) \rangle = \Phi_M(x) + \frac{1}{2} \left[1 + \operatorname{erf} \left(\frac{x - L_M}{2\sqrt{x\xi}} \right) \right] + \Phi_M(x) \pi \delta(E/\Delta_\xi). \quad (10)$$

The last δ term in Eq. (10) corresponds to the localized Majorana mode whose profile is given by

$$\Phi_M(x) = 2\pi \int_0^\infty k dk \frac{\sinh \pi k}{\cosh^2 \pi k} (k^2 + 1/4) e^{-(x/\xi)(k^2 + 1/4)}, \quad (11)$$

and

$$L_M = 2\xi \ln(\Delta_\xi/E) \quad (12)$$

is the Mott length scale [15]. Note that the profile of the Majorana level $\Phi_M(x)$ contributes not only to the

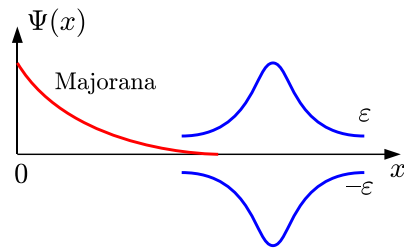


FIG. 3: (Color online) A schematic representation of the three localized states whose hybridization is responsible for $\langle \rho_E(x) \rangle$ at small, but finite energies E .

delta peak at zero energy, but also to the background LDOS at small finite energies (see our discussion of Mott hybridization below). The function $\langle \rho_E(x) \rangle$ is plotted in Fig. 2.

As in the short-wire limit, one can verify that the integral weight of the Majorana delta peak in the LDOS (10) equals $1/2$. The *average* intensity of the Majorana mode decays away from the interface at the length scale 4ξ , similar to the statistics of a single localized wave function [26, 28, 32]. On general grounds, we believe that the statistics of the tails of this localized state is log-normal [16] with the *typical* Majorana state decaying at the length scale ξ . Note however that the exact form of the average intensity of the Majorana state (11) differs from the two-point correlation function of the intensity of a single localized state [Eq. (75) of Ref. 28, see also Refs. 26, 32].

We can also remark a similarity of the LDOS profile (10) to the two-point LDOS correlation function in the quasi-one-dimensional wire [16, 28]. Namely, at low energies, it consists of two parts: the “short-range” part localized at the length scale ξ and proportional to the single-particle statistics [$\Phi_M(x)$ in our case] and the “long-range” part at the length scale L_M . As in the case of a quasi-one-dimensional wire, this structure may be easily understood in terms of a Mott hybridization of localized states. The difference from the two-point-correlation case considered in Ref. 16 is that now three states hybridize: the Majorana state and the pair of particle-hole (Bogoliubov–de-Gennes) symmetric [18, 20] states at energies ϵ and $-\epsilon$ (see Fig. 3). The hybridization Hamiltonian involving these three states has the form

$$H_{\text{hybrid}} = \begin{pmatrix} \epsilon & J & 0 \\ J^* & 0 & J^* \\ 0 & J & -\epsilon \end{pmatrix}, \quad (13)$$

where the *typical* value of the hybridization matrix element J is $\Delta_\xi e^{-x/(2\xi)}$ (note that there is no direct hybridization between the state at energy ϵ and its image in the symmetry class B [20]). Following the argument of Ref. 16, we conclude that this hybridization mechanism produces a crossover between $\rho_E(x) = 0$ and $\rho_E(x) = 1$ at $x = L_M$, in agreement with the result (10) of our cal-

TABLE I: Level repulsion and Mott hybridization in normal-metal–superconductor junctions of the symmetry classes B, D, and C in the limit of an infinite wire $L \rightarrow \infty$.

Class	Majorana	α	hybrid. length	$\langle \rho_{E \rightarrow 0}(0) \rangle$
B	Yes	2	$2\xi \ln(\Delta_\xi/E)$	1
D	No	0	—	3
C	No	2	$\xi \ln(\Delta_\xi/E)$	0

culuation. Following the same argument, the hybridized states reproduce the Majorana wave function at $x \lesssim \xi$, and therefore $\langle \rho_E(x) \rangle$ must be proportional to the average intensity of the Majorana state $\Phi_M(x)$ in this region of x , again in agreement with Eq. (10).

It is instructive to compare this situation with that in superconductor–normal-metal (SN) junctions in the symmetry classes C and D considered in Ref. 14. In class D, there is no hybridization between any state and its particle-hole mirror image [20]. Since there is no state at $E = 0$, this implies no repulsion from the Fermi level, and $\langle \rho_E(x) \rangle$ is enhanced at low energies at $x \lesssim \xi$ (with $\langle \rho_{E \rightarrow 0}(0) \rangle = 3$). In class C, the particle-hole mirror images hybridize and repel each other, and therefore $\langle \rho_E(x) \rangle$ is suppressed at $x < L_M/2$ (as opposed to $x < L_M$ in class B), since hybridization involves an electron (hole) propagating to the interface with the superconductor and back. The comparison of the three classes is presented in Table I.

We remark that finite limits $\langle \rho_{E \rightarrow 0}(x) \rangle$ in classes B and D reported in Table I are only achieved if the limit $L \rightarrow \infty$ is taken before $E \rightarrow 0$. If one considers the opposite order of limits, (i.e., $E \rightarrow 0$ at a finite L), then the repulsion from the Fermi level leads to $\langle \rho_{E \rightarrow 0}(x) \rangle = 0$. In fact, in a finite wire, the hybridization is only possible at distances $x < L$, which sets the energy scale $E_g \sim \Delta_\xi e^{-L/(2\xi)}$ in class B (whereas $E_g \sim \Delta_\xi e^{-L/\xi}$ in class C) as the typical minimum energy of hybridized states. Below this energy scale, the density of states is suppressed, which is reminiscent of a minigap in conventional SN junctions [33]. In a finite wire, at very small energies ($E \ll E_g$), the density of states scales as $\langle \rho_{E \rightarrow 0}(x) \rangle \propto |E|^\alpha$. A finite value of α indicates repulsion either from the Majorana state or from the Bogoliubov–de Gennes mirror image: it equals the number of independent degrees of freedom in the possible hybridization matrix element between the two repelling states. The values of α are included in Table I for completeness. They are also known from the random matrix theory for all symmetry classes (Refs. 12, 20, 29 and references therein).

6. Discussion.— To summarize, we have analytically solved the problem of Anderson localization of a Majorana fermion in a wire with time-reversal and spin-rotational symmetries broken. We find that the Majorana

level gets localized in a way qualitatively similar to other electronic states and contributes to the repulsion of other electron levels from the Fermi energy near the SN interface. We expect that these qualitative properties are universal: they do not depend on the details of geometry and on the symmetry class of the wire. Moreover, since the statistics of the envelope of a single localized wave function in quasi-one-dimensional geometry is independent of the symmetry class [34] and since the behavior at the Mott length scale is determined by the hybridization physics [15, 16], we believe that our results (10) and (11) are universally valid also for wires with orthogonal and symplectic symmetries, as long as a Majorana level is present at the SN interface.

Our results may be useful for possible qubit designs involving Majorana fermions localized by disorder. The intensity $\Phi_M(x)$ of the Majorana state may be probed by tunneling experiments (while the maximum of the tunneling peak at zero temperature must equal $2e^2/h$, according to Ref. 24, its width and temperature smearing are sensitive to the amplitude $\Phi_M(x)$ [25]). Also, the profile of $\Phi_M(x)$ would be relevant for hybridization of Majorana fermions, if two of them are placed at the opposite ends of the wire (similarly to the case of a superconducting wire considered in Ref. 35).

This work was partially supported by the program “Quantum mesoscopic and disordered structures” of the RAS, RFBR grant No. 13-02-01389, and the German Ministry of Education and Research (BMBF).

-
- [1] C. W. Beenakker, *Annu. Rev. Con. Mat. Phys.* **4**, 113 (2013).
Search for Majorana fermions in superconductors.
 - [2] V. Mourik, K. Zuo, S. M. Frolov, S. R. Plissard, E. P. A. M. Bakkers, and L. P. Kouwenhoven, *Science* **336**, 1003 (2012).
Signatures of Majorana fermions in hybrid superconductor-semiconductor nanowire devices.
 - [3] A. Das, Y. Ronen, Y. Most, Y. Oreg, M. Heiblum, and H. Shtrikman, *Nature Physics* **8**, 887 (2012).
Evidence of Majorana fermions in an Al-InAs nanowire topological superconductor.
 - [4] M. T. Deng, C. L. Yu, G. Y. Huang, M. Larsson, P. Caroff, and H. Q. Xu, *Nano Lett.* **12**, 6414 (2012).
Observation of Majorana fermions in a Nb-InSb Nanowire-Nb hybrid quantum device.
 - [5] L. P. Rokhinson, X. Liu, and J. K. Furdyna, *Nature Physics* **8**, 795 (2012).
Observation of the fractional ac Josephson effect: the signature of Majorana particles.
 - [6] A. R. Akhmerov, J. P. Dahlhaus, F. Hassler, M. Wimmer, and C. W. J. Beenakker, *Phys. Rev. Lett.* **106**, 057001 (2011).
Quantized conductance at the Majorana phase transition in a disordered superconducting wire.
 - [7] M. Wimmer, A. R. Akhmerov, J. P. Dahlhaus, and

- C. W. J. Beenakker, *New J. Phys.* **13**, 053016 (2011).
Quantum point contact as a probe of a topological superconductor.
- [8] J. Liu, A. C. Potter, K. T. Law, and P. A. Lee, *Phys. Rev. Lett.* **109**, 267002 (2012).
Zero-bias peaks in spin-orbit coupled superconducting wires with and without Majorana end-states.
- [9] D. I. Pikulin, J. P. Dahlhaus, M. Wimmer, H. Schomerus, and C. W. Beenakker, *New J. Phys.* **14**, 125011 (2012).
Zero-voltage conductance peak from weak antilocalization in a Majorana nanowire.
- [10] P. W. Anderson, *Phys. Rev.* **109**, 1492 (1958).
Absence of diffusion in certain random lattices.
- [11] M. Bocquet, D. Serban, and M. R. Zirnbauer, *Nucl. Phys. B* **578**, 628 (2000).
Disordered 2d quasiparticles in class D: Dirac fermions with random mass, and dirty superconductors.
- [12] D. A. Ivanov, *J. Math. Phys.* **43**, 126 (2002).
The supersymmetric technique for random-matrix ensembles with zero eigenvalues.
- [13] K. B. Efetov, *Adv. Phys.* **32**, 53 (1983).
Supersymmetry and theory of disordered metals.
- [14] M. A. Skvortsov, P. M. Ostrovsky, D. A. Ivanov, and Ya. V. Fominov, *Phys. Rev. B* **87**, 104502 (2013).
Superconducting proximity effect in quantum wires without time-reversal symmetry.
- [15] N. F. Mott, *Philos. Mag.* **17**, 1259 (1968).
Conduction in non-crystalline systems. I. Localized electronic states in disordered systems.
ibid. **22**, 7 (1970).
Conduction in non-crystalline systems. IV. Anderson localization in a disordered lattice.
- [16] D. A. Ivanov, M. A. Skvortsov, P. M. Ostrovsky, and Ya. V. Fominov, *Phys. Rev. B* **85**, 035109 (2012).
Hybridization of wave functions in one-dimensional localization.
- [17] C. W. Beenakker, J. P. Dahlhaus, M. Wimmer, and A. R. Akhmerov, *Phys. Rev. B* **83**, 085413 (2011).
Random-matrix theory of Andreev reflection from a topological superconductor.
- [18] M. R. Zirnbauer, *J. Math. Phys.* **37**, 4986 (1996).
Riemannian symmetric superspaces and their origin in randommatrix theory.
- [19] K. B. Efetov, *Supersymmetry in Disorder and Chaos* (Cambridge University Press, New York, 1997).
- [20] A. Altland and M. R. Zirnbauer, *Phys. Rev. B* **55**, 1142 (1997).
Nonstandard symmetry classes in mesoscopic normal-superconducting hybrid structures
- [21] R. M. Lutchyn, J. D. Sau, and S. Das Sarma, *Phys. Rev. Lett.* **105**, 077001 (2010).
Majorana fermions and a topological phase transition in semiconductor-superconductor heterostructures.
- [22] Y. Oreg, G. Refael, and F. von Oppen, *Phys. Rev. Lett.* **105**, 177002 (2010).
Helical liquids and Majorana bound states in quantum wires.
- [23] The $1/2$ factor in the definition of the level spacing δ takes into account the doubling of levels due to Andreev reflections and is included for consistency of notations with Refs. [12, 14, 20].
- [24] K. T. Law, P. A. Lee, and T. K. Ng, *Phys. Rev. Lett.* **103**, 237001 (2009).
Majorana fermion induced resonant Andreev reflection.
- [25] P. A. Ioselevich and M. V. Feigel'man, arXiv:1211.2722.
Tunneling conductance due to discrete spectrum of Andreev states.
- [26] K. B. Efetov and A. I. Larkin, *Zh. Eksp. Teor. Fiz.* **85**, 764 (1983) [*Sov. Phys. JETP* **58**, 444 (1983)].
Kinetics of a quantum particle in a long metallic wire.
- [27] D. A. Ivanov and M. A. Skvortsov, *J. Phys. A: Math. Theor.* **41**, 215003 (2008).
Dyson-Maleev representation of nonlinear sigma-models.
- [28] D. A. Ivanov, P. M. Ostrovsky, M. A. Skvortsov, *Phys. Rev. B* **79**, 205108 (2009).
Correlations of the local density of states in quasi-one-dimensional wires.
- [29] M. L. Mehta, *Random Matrices* (Academic Press, Boston, 1991).
- [30] M. A. Skvortsov and P. M. Ostrovsky, *Pis'ma v ZhETF* **85**, 79 (2007) [*JETP Lett.* **85**, 72 (2007)].
Local correlations of different eigenfunctions in a disordered wire.
- [31] See Supplemental Material.
- [32] A. A. Gogolin, *Zh. Eksp. Teor. Fiz.* **71**, 1912 (1976) [*Sov. Phys. JETP* **44**, 1003 (1976)].
Electron density distribution for localized states in a one-dimensional disordered system.
- [33] A. A. Golubov and M. Yu. Kupriyanov, *Zh. Eksp. Teor. Fiz.* **96**, 1420 (1989) [*Sov. Phys. JETP* **69**, 805 (1989)].
Josephson effect in SNINS and SNIS tunnel structures with finite transparency of the SN boundaries.
- [34] A. D. Mirlin, *J. Math. Phys.* **38**, 1888 (1997).
Spatial structure of anomalously localized states in disordered conductors.
A. D. Mirlin, *Phys. Rep.* **326**, 259 (2000).
Statistics of energy levels and eigenfunctions in disordered systems.
- [35] P. W. Brouwer, M. Duckheim, A. Romito, and F. von Oppen, *Phys. Rev. Lett.* **107**, 196804 (2011).
Probability distribution of Majorana end-state energies in disordered wires.

Supplemental Material

Here we provide the details of the calculation leading to the results (10) and (11) for the LDOS in the infinite-wire limit. The calculation extensively uses the techniques developed in Ref. 28. In the fermionic sector, the calculation is done perturbatively, while in the bosonic sector we use the Poisson summation formula involving the scattering matrix for the Hamiltonian \tilde{H}_B [Eq. (6a)]. It will be convenient to perform the calculation in the variables p and q introduced below Eq. (9). We also introduce the dimensionless coordinate $t = x/\xi$. The main idea of the calculation is to keep track of the relevant orders in κ .

The starting point of the calculation are Eqs. (3), (8), and (9). The Hamiltonians (6a) and (6b) in the variables p and q read

$$\tilde{H}_B = \frac{1}{8} \left[\frac{1}{p} \frac{\partial}{\partial p} p(\kappa^2 - p^2) \frac{\partial}{\partial p} + p^2 - \frac{\kappa^2}{2} \right], \quad (\text{S1})$$

$$\tilde{H}_F = \frac{1}{8} \left[\frac{1}{q} \frac{\partial}{\partial q} q(q^2 - \kappa^2) \frac{\partial}{\partial q} - q^2 + \frac{\kappa^2}{2} \right]. \quad (\text{S2})$$

In the fermionic sector, we expand the wave function in powers of κ and q :

$$\Psi(q, p; t) = \psi_0(p, t) + q^2 \psi_1(p, t) + \kappa^2 \psi_2(p, t) + \dots, \quad (\text{S3})$$

which, upon substitution into Eq. (3), results in

$$\langle \rho_E(x) \rangle = 1 + \frac{1}{2} \text{Re} \int d\lambda_B \left[2\psi_0(p, t) + \kappa^2 \psi_1(p, t) + 2\kappa^2 \psi_2(p, t) + \dots \right]. \quad (\text{S4})$$

The Hamiltonian \tilde{H}_F acts as

$$\begin{aligned} \tilde{H}_F [\psi_0 + q^2 \psi_1 + \kappa^2 \psi_2] \\ = (q^2 - \kappa^2/2) \left[-\psi_0/8 + \psi_1 \right] + o(q^2, \kappa^2), \end{aligned} \quad (\text{S5})$$

which allows us to represent it by a finite matrix in the basis $(1, q^2, \kappa^2)$:

$$\tilde{H}_F \begin{pmatrix} \psi_0 \\ \psi_1 \\ \psi_2 \end{pmatrix} = \begin{pmatrix} 0 & 0 & 0 \\ -1/8 & 1 & 0 \\ 1/16 & -1/2 & 0 \end{pmatrix} \begin{pmatrix} \psi_0 \\ \psi_1 \\ \psi_2 \end{pmatrix} + o(q^2, \kappa^2). \quad (\text{S6})$$

Exponentiating this matrix, we obtain

$$\begin{aligned} e^{-2\tilde{H}_F t} [\psi_0 + q^2 \psi_1 + \kappa^2 \psi_2] \\ = \psi_0 + q^2 \left[\frac{1 - e^{-2t}}{8} \psi_0 + e^{-2t} \psi_1 \right] \\ + \kappa^2 \left[\frac{e^{-2t} - 1}{16} \psi_0 + \frac{1 - e^{-2t}}{2} \psi_1 + \psi_2 \right] + o(q^2, \kappa^2). \end{aligned} \quad (\text{S7})$$

Applying this operation to the zero-mode wave function

$$\Psi_0(q, p) = pK_1(p) + q^2 \left(\frac{K_0(p)}{2} + \frac{pK_1(p)}{4} \right) + o(q^2) \quad (\text{S8})$$

yields

$$\begin{aligned} e^{-2\tilde{H}_F t} \Psi_0(q, p) &= pK_1(p) \\ &+ q^2 \left[\frac{1 + e^{-2t}}{8} pK_1(p) + \frac{e^{-2t}}{2} K_0(p) \right] \\ + \kappa^2 \left[\frac{1 - e^{-2t}}{16} pK_1(p) + \frac{1 - e^{-2t}}{4} K_0(p) \right] &+ o(q^2, \kappa^2). \end{aligned} \quad (\text{S9})$$

Inserting this result into Eq. (S4), we obtain

$$\begin{aligned} \langle \rho_E(x) \rangle &= 1 + \text{Re} \int d\lambda_B e^{-2\tilde{H}_B t} \left(pK_1(p) \right. \\ &\left. + \frac{\kappa^2}{8} [pK_1(p) + 2K_0(p)] \right). \end{aligned} \quad (\text{S10})$$

This equation is valid up to corrections of order $o(\kappa^2)$ in the integrand, which results in corrections of order $o(1)$ for $\langle \rho_E(x) \rangle$ (the integration over λ_B extends to $\lambda_B \sim \kappa^{-2}$ and thus brings in a large κ^{-2} factor). It remains now to calculate the evolution with respect to the bosonic part of the Hamiltonian \tilde{H}_B .

We further calculate the following two matrix elements

$$\begin{Bmatrix} M_1 \\ M_0 \end{Bmatrix} = \int d\lambda_B e^{-2\tilde{H}_B t} \begin{Bmatrix} pK_1(p) \\ K_0(p) \end{Bmatrix} \quad (\text{S11})$$

using the method developed in Ref. 28. From Eq. (S10) we see that the integral involving $pK_1(p)$ should be calculated up to two leading terms in small energy expansion, $O(1/\kappa^2)$ and $O(1)$, while for the second integral it suffices to extract only the main $O(1/\kappa^2)$ asymptotics.

We use the general expansion of the evolution operator in the eigenfunctions of \tilde{H}_B

$$\begin{Bmatrix} M_1 \\ M_0 \end{Bmatrix} = \sum_k \frac{\langle 1 | \phi_k \rangle}{\langle \phi_k | \phi_k \rangle} e^{-2E_k t} \begin{Bmatrix} \langle \phi_k | pK_1(p) \rangle \\ \langle \phi_k | K_0(p) \rangle \end{Bmatrix} \quad (\text{S12})$$

and pick all the necessary ingredients from Ref. 28:

$$\langle \phi_k | p K_1(p) \rangle = \frac{\pi}{\kappa \cosh \pi k} \left[1 + 4k^2 - \frac{\kappa^2}{2} + O(\kappa^4) \right], \quad (\text{S13})$$

$$\langle \phi_k | K_0(p) \rangle = \frac{2\pi}{\kappa \cosh \pi k} [1 + O(\kappa^4)], \quad (\text{S14})$$

$$\langle \phi_k | \phi_k \rangle = -\frac{i}{2\pi} \coth \pi k \frac{\partial \ln S(k)}{\partial k} \left[\frac{1}{k} + O(\kappa^4) \right], \quad (\text{S15})$$

$$\sum_k \dots = -\frac{i}{2\pi} \sum_{n=-\infty}^{+\infty} \int_0^\infty dk S^n(k) \frac{\partial \ln S(k)}{\partial k} \dots, \quad (\text{S16})$$

$$S(k) = \left(\frac{\kappa^2}{4} \right)^{-2ik} \left[\frac{\Gamma(2ik)\Gamma(1/2 - ik)}{\Gamma(-2ik)\Gamma(1/2 + ik)} \right]^2 \times [1 + O(\kappa^4)], \quad (\text{S17})$$

$$E_k = \frac{1}{8} + \frac{k^2}{2} + O(\kappa^4). \quad (\text{S18})$$

The only missing piece is $\langle 1 | \phi_k \rangle$. It can be easily computed along the lines of Appendix C of Ref. 28:

$$\langle 1 | \phi_k \rangle = \int d\lambda_B \phi_k = \frac{4}{\kappa} [1 + O(\kappa^4)]. \quad (\text{S19})$$

Putting everything together, we obtain

$$M_1 = 4\pi \int_0^\infty k dk \frac{\sinh \pi k}{\cosh^2 \pi k} \sum_{n=-\infty}^{+\infty} S^n(k) \times \left[\frac{1 + 4k^2}{\kappa^2} - \frac{1}{2} + O(\kappa^2) \right] e^{-t(k^2+1/4)}. \quad (\text{S20})$$

The term with $n = 0$ rapidly converges as an integral over real k , while $n = \pm 1$ terms oscillate and are determined by the competition between the contributions of the pole at $k = i/2$ and of the saddle point $k_* = it_M/2t$ with $t_M = 4 \ln(2/\kappa)$. The pole contribution is dominant at $t \ll t_M$ and yields -1 . The saddle point k_* becomes important at $t \sim t_M$ and provides a step-like ‘‘erf term’’. The result is

$$M_1 = -\frac{1}{2} + \frac{1}{2} \operatorname{erf} \left(\frac{t - t_M}{2\sqrt{t}} \right) + 4\pi \int_0^\infty k dk \frac{\sinh \pi k}{\cosh^2 \pi k} \left[\frac{1 + 4k^2}{\kappa^2} - \frac{1}{2} \right] e^{-t(k^2+1/4)} + O(\kappa^2). \quad (\text{S21})$$

Evolution of $K_0(p)$ is easier since we need only the leading term. Setting $n = 0$, we find

$$M_0 = \frac{8\pi}{\kappa^2} \int_0^\infty k dk \frac{\sinh \pi k}{\cosh^2 \pi k} e^{-t(k^2+1/4)} + O(1). \quad (\text{S22})$$

The results (10) and (11) for the LDOS are now obtained in a straightforward way by substituting the integrals (S21) and (S22) into Eq. (S10). The Majorana delta peak arises from $\operatorname{Re}(1/\kappa^2) = (\pi/8)\delta(E/\Delta_\xi)$.